J. Plasma Physics (2015), *vol.* 81, 345810203 © Cambridge University Press 2014
doi:10.1017/S0022377814001172

Inverse mirror plasma experimental device (IMPED) – a magnetized linear plasma device for wave studies

Sayak Bose[1]†, P. K. Chattopadhyay[1], J. Ghosh[1], S. Sengupta[1], Y. C. Saxena[1] and R. Pal[2]

[1]Institute for Plasma Research, Bhat, Gandhinagar, Gujarat 382428, India
[2]Saha Institute of Nuclear Physics, 1/AF Bidhannagar, Kolkata 700064, India

(Received 21 August 2014; revised 17 October 2014; accepted 2 November 2014; first published online 8 December 2014)

In a quasineutral plasma, electrons undergo collective oscillations, known as plasma oscillations, when perturbed locally. The oscillations propagate due to finite temperature effects. However, the wave can lose the phase coherence between constituting oscillators in an inhomogeneous plasma (phase mixing) because of the dependence of plasma oscillation frequency on plasma density. The longitudinal electric field associated with the wave may be used to accelerate electrons to high energies by exciting large amplitude wave. However when the maximum amplitude of the wave is reached that plasma can sustain, the wave breaks. The phenomena of wave breaking and phase mixing have applications in plasma heating and particle acceleration. For detailed experimental investigation of these phenomena a new device, inverse mirror plasma experimental device (IMPED), has been designed and fabricated. The detailed considerations taken before designing the device, so that different aspects of these phenomena can be studied in a controlled manner, are described. Specifications of different components of the IMPED machine and their flexibility aspects in upgrading, if necessary, are discussed. Initial results meeting the prerequisite condition of the plasma for such study, such as a quiescent, collisionless and uniform plasma, are presented. The machine produces $\delta n_{noise}/n \leqslant 1\%$, $L_{uniform} \sim 120\,\mathrm{cm}$ at argon filling pressure of $\sim 10^{-4}$ mbar and axial magnetic field of $B = 1090\,\mathrm{G}$.

1. Introduction

Electrostatic plasma oscillation is one of the fundamental modes in plasma where the electrons oscillate with a frequency close to electron plasma frequency (ω_{pe}). Here, a high frequency longitudinal density oscillation is excited when quasineutrality of the plasma is violated locally. Tonks and Langmuir (1929) experimentally observed this oscillation and provided a basic theoretical explanation; however, they restricted their treatment to cold plasma and small amplitude oscillation. The effect of thermal motion of particles was studied theoretically by Vlasov and Landau. Landau (1946), in fact, showed that it is possible to damp electron plasma waves even without collision. A physical picture of this Landau damping was later given by Dawson (1961) who explained the phenomena as exchange of energy between the wave and the particles having velocity close to wave phase velocity (resonant wave–particle interaction).

† Email address for correspondence: sayak@ipr.res.in

https://doi.org/10.1017/S0022377814001172 Published online by Cambridge University Press

Experimentally Malmberg et al. (1966) established the collisionless damping of electron plasma wave. They measured the spatial damping of longitudinal electron plasma wave, excited by applying a high frequency voltage to a Langmuir probe in a collisionless plasma. The authors also verified the role of resonant electrons in the collisionless damping by cutting off the tail of the Maxwell distribution of electrons and observed a sharp decrease in damping. O'Neil (1965) extended the damping of collisionless nonlinear plasma oscillations to time (t) greater than $\tau_B(=\sqrt{m/eEk})$, the bounce period of the trapped particles in the wave having electric field amplitude E and wave number k. The damping coefficient has an oscillatory behavior when t/τ is of the order of unity, and it phase mixes to zero as $t/\tau \to \infty$. This nonlinear behavior of the damping coefficient was experimentally proven by Malmberg and Wharton (1967). They investigated the damping of a large amplitude plasma wave and observed amplitude oscillation at large distances from the exciter. In the course of their experiment, Wharton et al. (1968) observed side bands separated from the transmitter frequency by bounce frequency $\omega_B\,(=1/\tau_B)$ associated with large amplitude electron plasma wave. Subsequently, different aspects of nonlinear electron plasma wave, namely, electron trapping effects, wave–wave interaction and side band instability, were investigated by Franklin et al. (1975a,b, 1978)

It is observed that on increasing the amplitude of electron plasma wave, different nonlinear effects become dominant. But plasma does not sustain wave having arbitrarily high amplitude, and beyond certain limit wave breaks. The maximum electric field amplitude that a plasma can sustain is a topic of fundamental importance to many areas of plasma physics particularly, plasma based particle acceleration schemes (Tajima and Dawson 1979; Esarey et al. 2009) and some laser fusion schemes (Tabak et al. 1994; Kodama et al. 2001). In laser fusion experiments, energetic electrons generated by wave breaking eventually leads to heating of the core and in plasma based particle accelerators, the maximum energy of the particles accelerated by resonant wave–particle interaction is dictated by the wave breaking amplitude. In cold plasma, wave breaking occurs when the electron excursion length becomes comparable to the wavelength and which is characterized by sharp rise in the local electron density and its gradient (Dawson 1959). Bauer et al. (1992) reported experimental observation of wave breaking of electron plasma wave in a radiofrequency (RF) afterglow plasma. They observed energetic electrons associated with wave breaking. Electron acceleration in the relativistic regime from the breaking of plasma waves was reported by Modena et al. (1995).

Besides wave breaking, a wave may lose its coherence by another less violent process namely phase mixing of plasma oscillation/wave. Phase mixing is the loss of coherence of plasma oscillation/wave due to fine scale mixing of various parts of the oscillation/wave when there is a spatial variation of local plasma frequency. This can happen due to presence of inhomogeneity in the background plasma density that may occur due to a number of reasons (Kaw et al. 1973; Sengupta and Kaw 1999; Sengupta et al. 2011). The concept of phase mixing of wave in an inhomogeneous medium leading to dissipation of wave energy serves as a possible model of coronal heating. Alfven wave phase mixing in a medium with a density gradient perpendicular to the magnetic field has been studied as a possible mechanism for coronal heating (Botha et al. 2000).

So, it appears that some experiments have been carried out to observe and characterize wave breaking phenomena, but a comprehensive study testing various predictions of theory and simulation is far from satisfactory. Recently Verma et al. (2012) using one dimensional particle in cell simulation of large amplitude plasma

https://doi.org/10.1017/S0022377814001172 Published online by Cambridge University Press

oscillations in cold plasma showed the excitation of residual Bernstein–Greene–Kruskal like waves after electron wave breaking in cold plasma. The amplitude of the residual BGK wave satisfies the Coffey's wave breaking limit for warm plasma (Coffey 1971). Such theoretically predicted results, where the plasma heats up after electron plasma wave breaking and eventually supports a BGK like wave with an amplitude limit determined by Coffey's limit (Coffey 1971) needs to be experimentally verified. Further it is well known that electron plasma oscillations break via the process of wave breaking in an inhomogeneous plasma (Dawson 1959; Infeld et al. 1989). It has been theoretically predicted that collisions can possibly prevent the breaking of waves (de Nicola and Nappi 1992). This is another theoretical result whose experimental verification, to the best of our knowledge, does not exist. With these perspective in mind a new machine, IMPED, has been designed and fabricated in house at Institute for Plasma Research, India, where phase mixing and wave breaking of nonlinear plasma oscillation/wave will be investigated comprehensively in a controlled manner. In IMPED, production of quiescent, collisionless, and magnetized plasma has been achieved over a wide range of operating parameters. Lowest operating pressure for argon plasma is 1.7×10^{-5} mbar. The density and temperature are varied from 10^9 to $10^{12}\,\mathrm{cm}^{-3}$ and 2 to 5 eV, respectively. The plasma produced is axially uniform over 120 cm and radially uniformity is typically 4 cm. The system has the option of varying radial uniformity. The procedure adopted for designing the device in order to ensure that different aspects of phase mixing and wave breaking of plasma oscillation/wave can be investigated experimentally, is described in details in this article.

In this paper, in Sec. 2 the phenomena of wave breaking and phase mixing of nonlinear plasma oscillation/wave have been discussed. In Sec. 3, the operating window has been determined where the phase mixing is expected to be dominant compared to other processes namely collisional damping and linear Landau damping. In Sec. 4, selection of plasma source on the basis of the experimental requirement has been presented. This has been followed by description of IMPED and discussions on its initial results in Sec. 5. Finally in Sec. 6, we summarize the discussions on the system and point out future possibilities.

2. Theoretical background: phase mixing and wave breaking of nonlinear plasma oscillation

IMPED has been designed for experimental investigation of phase mixing and wave breaking of nonlinear plasma oscillation/wave in a cold homogeneous plasma. A plasma oscillation/wave breaks when the electron excursion length becomes of the order of plasma wavelength i.e. $keE/m\omega_{pe}^2 \sim 1$, or in other words the oscillation/wave breaks when fluid velocity $(eE/m\omega_{pe})$ becomes of the order of the phase velocity (ω_{pe}/k). Physically this results in the crossing of neighboring electron trajectories. At the point of breaking intense wave–particle interaction occurs resulting in transfer of energy from the wave to random particle kinetic energy. A plasma oscillation/wave may break suddenly when it is excited in a way such that the breaking condition is satisfied within a plasma period or it may occur gradually through a process known as phase mixing.

Phase mixing of an oscillation/wave implies decay of the oscillation/wave by fine scale mixing of various parts of the oscillation due to temporal dependence of the phase difference between individual oscillators constituting the oscillation/wave. This temporal dependence of the phase difference between oscillating fluid elements arises, when the plasma frequency because of some physical reason acquires a spatial

https://doi.org/10.1017/S0022377814001172 Published online by Cambridge University Press

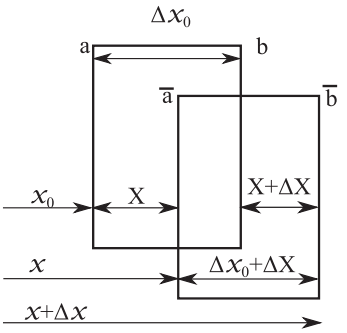


FIGURE 1. One dimensional sheet model describing plasma oscillation.

dependence. Phase mixing eventually results in crossing of electron trajectories thus causing the oscillation/wave to break. Spatial dependence of plasma frequency, which is the underlying cause of phase mixing may arise either due to the presence of a static inhomogeneous background (infinitely massive ions, as discussed in Dawson (1959) (Kaw et al. 1973; Infeld et al. 1989; Infeld and Rowlands 1990) or due to gradual development of an inhomogeneity which results from the excitation of a low frequency self-consistent field in the presence of finite ion mass background (Sengupta and Kaw 1999). In the presence of a static inhomogeneity, Dawson (1959) showed that cold plasma oscillations phase mix at arbitrarily small amplitudes in a time scale given by $t_{mix} \sim \pi/\{2(d\omega_{pe}/dx)X\}$, where X is the displacement from the equilibrium position. For a sinusoidal inhomogeneity ($n_i = n_0 + n_0 \epsilon cosk_i x$), the phenomenon of phase mixing in the form of mode coupling of a long wavelength mode to short wavelength modes was discussed by Kaw et al. (1973), who showed that energy irreversibly goes from the low 'k' mode to high 'k' modes in a time scale $t_{mix} \sim 2/(\epsilon\omega_{pe})$. The exact solution for cold plasma oscillations in a fixed sinusoidal background was given by Infeld et al. (1989) who described phase mixing in term of electron density burst. As stated above, inhomogeneity in the background may also gradually arise in a homogeneous plasma in the presence of nonlinear plasma oscillations due to the response of the background species to ponderomotive forces either directly or through low frequency self-consistent fields (Sengupta and Kaw 1999). For this case, it has been shown that plasma oscillations phase mix in a time scale $\omega_{pe}t_{mix} \sim \{(A^2/24)(\Delta/\sqrt{1+\Delta})\}^{-1/3}$, where $A = \delta n/n$ and $\Delta = m_e/m_+$.

In the following subsections we briefly illustrate the physics of wave breaking and phase mixing (resulting in breaking) using a physically intuitive sheet model proposed by Dawson (1962).

2.1. *Wave breaking of nonlinear plasma oscillations*

Dawson (1962) proposed a one dimensional sheet model. According to which evolution of any coherent mode in a plasma can be studied in terms of oscillating motion of electron sheets about their equilibrium positions. These electron sheets are assumed to be embedded in a cold immobile positive ion background. Dawson (1959) showed that a coherent mode will maintain its coherence provided the electron sheets, while oscillating, do not cross each other. Crossing of electron sheets leads to a phenomenon called wave breaking which completely destroys the coherence of the wave.

Consider the adjoining Fig. 1. Let the electron originally placed at an equilibrium position x_0 be displaced by an amount $X(x_0, t)$ and the electron originally at the

https://doi.org/10.1017/S0022377814001172 Published online by Cambridge University Press

equilibrium position $x_0 + \Delta x_0$ be displaced by $X + \Delta X$. Here x_0 is the Lagrange coordinate of the electron. Equating the number of electrons originally contained between Δx_0 to the number of electrons contained between $\Delta x_0 + \Delta X$, we get the electron density as

$$n(x_0, t) = \frac{n_0}{\left[1 + \frac{\partial X(x_0,t)}{\partial x_0}\right]}, \tag{2.1}$$

where n_0 is the equilibrium number density. Further, the width of the ion slab crossed by the electron sheet which was originally at x_0 is X, which by using Gauss's law, yields the electric field as

$$E(x_0, t) = \frac{n_0 e}{\epsilon_0} X(x_0, t). \tag{2.2}$$

Therefore, the equation of motion of the electron sheet can now be written as

$$\begin{aligned} m\ddot{X} &= -eE \\ &= -\frac{n_0 e^2}{\epsilon_0} X, \end{aligned} \tag{2.3}$$

which finally gives

$$\ddot{X} + \omega_{pe}^2 X = 0, \tag{2.4}$$

where ω_{pe} is the plasma frequency. This is the equation of motion for a simple harmonic oscillator whose general solution has the form

$$X(x_0, t) = X(x_0, 0) cos(\omega_{pe} t) + \frac{V(x_0, 0)}{\omega_{pe}} sin(\omega_{pe} t). \tag{2.5}$$

In order to study nonlinear plasma oscillation and its breaking, we use the following initial conditions, which in terms of Euler coordinates x are given by

$$n(x, 0) = n_0(1 + \Delta cos(kx)) \tag{2.6}$$

$$v(x, 0) = 0, \tag{2.7}$$

where the Euler coordinate x is related to Lagrange coordinate x_0, as $x = x_0 + X(x_0, t)$. The above initial conditions immediately lead to

$$X(x_0, t) = X(x_0, 0) cos(\omega_{pe} t), \tag{2.8}$$

which when substituted in (2.1) gives the number density as

$$n(x_0, t) = \frac{n_0}{\left[1 + \frac{\partial X(x_0,0)}{\partial x_0} cos(\omega_{pe} t)\right]}. \tag{2.9}$$

Here $X(x_0, 0)$ is implicitly obtained by using (2.6) in Gauss's law and equating it to the electric field at $t = 0$ (given by (2.2)), as

$$X(x_0, 0) = -\frac{\Delta}{k} sin(k\tilde{x_0}), \tag{2.10}$$

where $\tilde{x_0} = x_0 + X(x_0, 0)$. For the density to remain positive at all times (or in other words, for no sheet crossing),

$$\frac{\partial X(x_0, 0)}{\partial x_0} cos(\omega_{pe} t) > -1. \tag{2.11}$$

https://doi.org/10.1017/S0022377814001172 Published online by Cambridge University Press

Using (2.10), the no-crossing condition now stands as

$$\frac{\Delta cos(k\tilde{x_0})}{1+\Delta cos(k\tilde{x_0})} cos(\omega_{pe}t) < 1. \tag{2.12}$$

The maximum value of the l.h.s is $\Delta/(1-\Delta)$, which gives $\Delta < 1/2$ for sustained coherent nonlinear oscillations. Hence in terms of electric field, the maximum value is limited to $keE_{max}/m\omega_{pe}^2 = \Delta < 1/2$ (Davidson 1972). Therefore, if the initial conditions are such that $\Delta \geqslant 1/2$, then cold plasma oscillations break within a plasma period, at an amplitude $E_{max} = m\omega_{pe}^2/2ke$. In the next subsection, we consider the case, where wave breaking occurs at arbitrarily low amplitudes via the phase mixing process.

2.2. *Phase mixing of nonlinear plasma oscillations*

As mentioned in the beginning of this section, plasma oscillations phase mix and eventually break if the plasma frequency becomes spatially dependent. Spatial dependence arises because of a background inhomogeneity, which in turn, may either be a static ion inhomogeneity or may arise self-consistently in the presence of electron–ion oscillations. As the electrons and ions move about their out own center of mass, they eventually create a low frequency electrostatic field, which further affects the motion of ions thus creating inhomogeneities in space. This in turn affects the electron wave motion causing it to phase mix. In this subsection, we illustrate the phase mixing phenomenon using a static background inhomogeneity. Taking a sinusoidal inhomogeneity as $n_i = n_0(1+\epsilon cos(k_i x_0))$, $\epsilon \ll 1$ (2.4) approximately becomes (taking $k_i X \ll 1$)

$$\ddot{X}(x_0,t) + \omega_{pe0}^2(1+\epsilon sin(k_i x_0))X(x_0,t) \approx 0. \tag{2.13}$$

Choosing $n_e = n_0(1+\epsilon cos(k_i x_0)) + \delta n_0 cos(k_e x)$ and $v(x,0) = 0$ ($k_e \ll k_i$) as initial conditions (Kaw et al. 1973), solution of the above equation can be written as

$$X(x_0,t) = X(x_0,0)cos(\omega_{pe0}t\sqrt{1+\epsilon sin(k_i x_0)}), \tag{2.14}$$

where $X(x_0,0)$ is approximately given by

$$X(x_0,0) \approx -\frac{\delta sin(k_e x_0)}{k_e(1+\epsilon sin(k_i x_0)+\delta cos(k_e x_0))}. \tag{2.15}$$

For $\epsilon \ll 1$, (2.14) can be further approximated as

$$X(x_0,t) \approx -\frac{\delta}{2k_e}\sum_{-\infty}^{\infty} J_n\left(\frac{\epsilon\omega_{pe0}t}{2}\right)[sin\{\omega_{pe0}t+(nk_i+k_e)x_0\} - sin\{\omega_{pe0}t+(nk_i-k_e)x_0\}]. \tag{2.16}$$

Since the electric field is directly related to $X(x_0,t)$ as

$$E(x_0,t) = \frac{m\omega_{pe0}^2}{e}(1+\epsilon sin(k_i x_0))X(x_0,t), \tag{2.17}$$

(2.16) shows that the field energy put in the fundamental mode diminishes as $\sim J_0^2(\epsilon\omega_{pe0}t/2)$ and the coherence is lost in a time scale $t_{mix} \sim 2/(\epsilon\omega_{pe0})$ (Kaw et al. 1973). Physically, since each electron sheet oscillates with a frequency which depends on its position, as time progresses, they slowly go out of phase and the initial coherence is lost. As energy goes into higher and higher modes, the density profile becomes more and more steep, eventually resulting in crossing of trajectories of neighboring electron sheets which causes the oscillations to break.

https://doi.org/10.1017/S0022377814001172 Published online by Cambridge University Press

The nonlinear problem of plasma oscillations in a static periodic ion background was exactly solved by Infeld et al. (1989) who analytically showed that, because of the spatial dependence of the plasma frequency, the electron number density will eventually explode. This is nothing but a signature of wave breaking. Thus the phenomenon of phase mixing ultimately causes the oscillations/waves to break at arbitrarily low amplitudes. If the inhomogeneity is self-consistently generated, then as stated above, plasma oscillations phase mix (wave break) in a time scale $\omega_{pe}\tau_{mix} \sim \{(A^2/24)(\Delta/\sqrt{1+\Delta})\}^{-1/3}$. Here A is the amplitude of perturbation and Δ is the electron to ion mass ratio.

3. Identification of the window of operation

Phase mixing is a gradual process. It happens over several plasma periods. In addition to phase mixing a wave may be lost in the plasma due to collisional damping and Landau damping. So it is necessary to find out the range of experimental parameters over which phase mixing of nonlinear plasma oscillations may be expected to dominate over other competing processes i.e. the phase mixing length is less than collisional damping or Landau damping length. In the following, we will estimate the maximum length within which phase mixing is expected to occur as well as all different length scales of the relevant damping mechanisms. From these calculations one arrives at the suitable plasma parameters the device should provide.

3.1. *Phase mixing length*

The maximum length within which phase mixing is expected to occur for various plasma densities and temperatures are determined from the expression: $\lambda_{mix} = t_{mix} v_{the}$.

The expression for t_{mix} is valid for electron plasma oscillation in a uniform background. For non-uniform background or in the presence of ion wave phase mixing length is even lower. From the expression for maximum phase mixing length it is obvious that its a function of plasma density, electron temperature, fluctuation level ($A = \delta n/n$) and electron to ion mass ratio Δ. As the plasma density increases the phase mixing length decreases. A plot of the variation of the maximum phase mixing length with change in A is given in Fig. 2 with different values of T_e. From the figure it is seen that for $A = 0.05$ the maximum λ_{mix} is 0.94 m at $T_e = 5$ eV and $n = 5 \times 10^8$ cm^{-3}. Hence from the perspective of maximum phase mixing length, operation at densities greater than 5×10^8 cm^{-3} is preferred, as for lower densities phase mixing length will increase. For example for same parameters as mentioned above, the maximum phase mixing length is 2.94 m for electron density of 5×10^7 cm^{-3}. For higher densities, say, 10^{10} cm^{-3}, the maximum phase mixing length will be much less, but with increase in density the plasma frequency also increases ($f_{pe} \propto \sqrt{n}$) thus increasing the demand on diagnostics. Thus the density window from mid 10^8 cm^{-3} to mid 10^9 cm^{-3} is preferred for the phase mixing experiment. The plasma temperature (T_e) should be around few eV, as for large T_e the maximum phase mixing length increases considerably. This is so because as the temperature increases the group velocity of the wave also increases thus increasing the phase mixing length.

3.2. *Collisional damping*

Experimental study on phase mixing requires all collision lengths to be greater than the maximum phase mixing length. This implies that the plasma has to be collisionless in order to observe the phase mixing phenomena. To ensure this the electron-neutral mean free path λ_{mf} ($= \frac{1}{n_n \sigma}$, n_n = neutral density and σ = electron-neutral collision crosssection), which is the dominant collision mechanism in laboratory plasmas,

https://doi.org/10.1017/S0022377814001172 Published online by Cambridge University Press

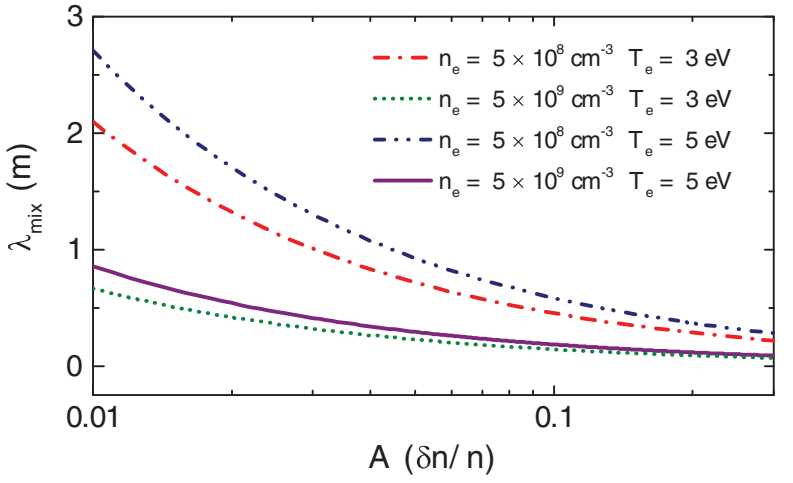


FIGURE 2. Varition of maximum phase mixing length with fluctuation $A = \frac{\delta n}{n}$ for argon plasma of different density and temperature.

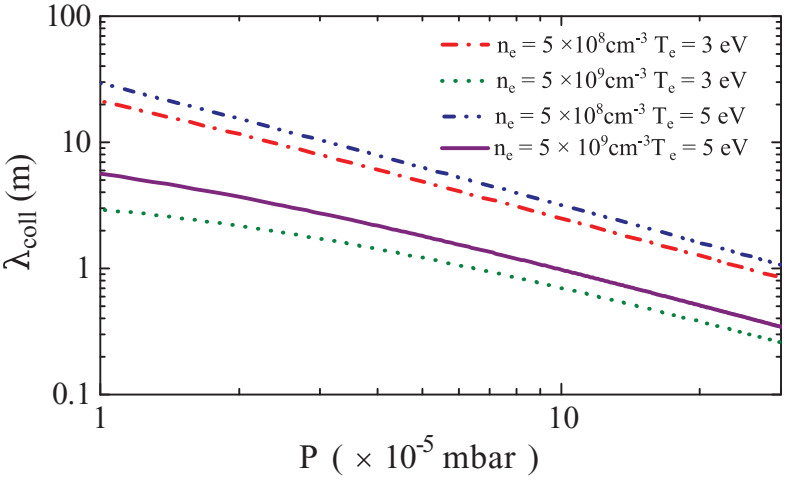


FIGURE 3. Variation of collisional damping length of linear Langmuir wave of wavelength 2.5 cm with pressure for different plasma densities and temperature.

must be several times the maximum phase mixing length. To get an estimate of the collisional damping length one may calculate the damping length of linear Langmuir wave. The formula for determining collisional damping length, λ_{coll}, of linear Langmuir wave in presence of both electron-neutral (ν_{en}) and electron–ion collision (ν_{ei}) is given by

$$\lambda_{coll} = \frac{2}{\nu_{ei} + \nu_{en}} \frac{\frac{3}{2} v_{the}^2 k}{\sqrt{\left\{\omega_p^2 + \frac{3}{2} v_{the}^2 k^2 - \frac{(\nu_{ei}+\nu_{en})}{4}\right\}}}. \tag{3.1}$$

Figure 3 shows the variation of the collisional damping length of a linear Langmuir wave having wavelength of 2.5 cm for different plasma parameters.

https://doi.org/10.1017/S0022377814001172 Published online by Cambridge University Press

From the figure it may be concluded that an operating pressure below 8×10^{-5} mbar is most suitable for operation. However experiments may be carried out at 1×10^{-4} mbar by exciting a higher density perturbation of $A > 0.08$.

3.3. *Landau damping length*

The phase mixing length should be less than the Landau damping length. The Landau damping length of the wave can be increased, by increasing the wavelength of the wave. This may be achieved by exciting the wave near the plasma frequency. Landau damping for a wave exhibiting weak damping (Franklin et al. 1975a) may be estimated by

$$k_i = \gamma_L \left(\frac{\partial \omega}{\partial k} \right)^{-1}, \tag{3.2}$$

where γ_L is the linear Landau damping rate in the time domain.

3.4. *Desirable features of plasma*

Based on the discussions as given above we now arrive at the most suitable features of the plasma that are necessary for observing phase mixing and wave breaking phenomena in laboratory. They are listed as follows:

(a) **Quiescence**: Ideally one would require a plasma with background fluctuation level $\delta n_{noise}/n$ much less than the perturbation level that is going to be excited. Hence one would require a quiet plasma. Taking practical difficulties into consideration, this background level should be $\leqslant 0.01$ at least.

(b) **Uniformity**: The plasma must be uniform, as phase mixing of nonlinear oscillation as per the route described by Sengupta and Kaw (1999) requires uniform plasma to begin with. The length of the uniform plasma must be greater than the maximum phase mixing length. Considering that the maximum phase mixing length for $A = 0.05$ in 5 eV argon plasma having density 5×10^8 cm^{-3} is 0.94 m. So, the uniform plasma length must be greater than 0.94 m.

(c) **Axial magnetic field**: One way of ensuring uniform plasma of length greater than 0.94 m is to use an axial magnetic field for confinement. The addition of magnetic field further enriches the wave phenomena that one may look at experimentally. Hence a variability of the magnetic field such that one may vary ω_{ce} from less than ω_{pe} to greater than ω_{pe} is desired.

(d) **Compatibility with different ion species**: The maximum phase mixing length is a function of the electron–ion mass ratio (Δ). This implies that in order to experimentally investigate the parametric dependence of the phase mixing time on Δ, one requires a plasma source compatible with different ion species.

4. Choice of plasma source

Keeping in mind the desired plasma features as outlined above a number of plasma sources were surveyed to meet the requirements. Not all of them are found to be suitable. For example, glow discharge plasma can have temperature in the range 1–5 eV and density 10^8– 10^{10} cm^{-3}. But one cannot have a collisionless plasma in this method since the operating pressure here is typically $>10^{-3}$ mbar and so the neutral density is very high. In addition, the plasma there is not quiescent.

A Q machine (Rynn and D'Angelo 1960) can be used to produce quiescent magnetized plasma ($B_0 \sim$ few kG), but since the electron temperature there is $\sim$0.2 eV, an electron density of 10^7–10^8 cm^{-3} is preferable for operation. The diameter of

https://doi.org/10.1017/S0022377814001172 Published online by Cambridge University Press

the uniform plasma can be controlled by the diameter of the hot plate and plasmas over a large length can be maintained using strong axial magnetic field. But in Q machine the ion species, which are alkali metal ions, cannot be changed easily, and technical complexities involved are large.

RF plasma sources generally have large density fluctuations, hence are not selected for operation. Duoplasmatron can be used to produce a long plasma column (>1 m) in the presence of a strong axial magnetic field of value of few kG at low pressures $\sim 10^{-5}$ mbar (Boeschoten and Schwirzke 1962). Plasma having density 10^8–10^9 cm^{-3}, temperature 5–20 eV using a duoplasmatron source have been reported in the literature (Malmberg et al. 1966). But the radial uniformity of the plasma produced using duoplasmatron is poor (Chen 1962).

Filament produced plasma is generally quiescent, but the lowest operating pressure for a filament plasma is $\sim 10^{-4}$ mbar. Plasma production using filaments in the presence of multicusp confinement can drastically lower the operating pressure. (Limpaecher and MacKenzie 1973) reported a lowest operating pressure of 5×10^{-6} mbar. Typical plasma parameters reported by them are 8×10^{10} cm^{-3}, $T_e = 5$ eV and $\delta n_{noise}/n \approx 2 \times 10^{-4}$. But any filament source is not compatible with an axial magnetic field. Gekelman and Stenzel (1975) developed a magnetized plasma device ($B_0 = 1$kG) with a multifilamentary source named SCAMP. The plasma produced is quiescent, axially and radially uniform. The lowest operating pressure of SCAMP is 5×10^{-5} torr. Considering that the filament plasma source is compatible with a number of filling gases, like, argon, krypton, xenon etc., so we find this kind of plasma source satisfies our criteria.

5. IMPED: its components

A new machine called IMPED has been designed and constructed taking into consideration all the different aspects that we discussed so far for carrying out experimental investigations of phase mixing and wave breaking phenomena of nonlinear plasma oscillation/wave in a cold homogeneous plasma. A schematic diagram of the machine is given in Fig. 5. The machine description of IMPED is presented here in five subsections: (a) the plasma source in Subsection 5.1, (b) the vacuum vessel in Subsection 5.2, (c) the magnet system in Subsection 5.3, (d) the diagnostics in Subsection 5.4, and (e) initial results of IMPED in Subsection 5.5.

5.1. *Plasma source*

Multifilamentary plasma source compatible with an axial magnetic field is used for plasma production. The plasma source is a two dimensional array of filaments located in the low magnetic field region. Thermionically emitted electrons by Joule heated filaments located in the low magnetic field region are accelerated by applying an accelerating voltage to the filaments. Plasma is produced by electron impact ionization. The plasma diffuses along the field line from the low magnetic field of the source chamber to the high magnetic field of the main plasma chamber. Because of the convergent geometry of the field line some of the charge particles may suffer reflection on its way to the main plasma chamber due to the magnetic mirror effect. In order to reduce loss of the charge particles on the source flange, the walls of the source flange are lined with permanent magnets in line cusp configuration. Two NdFeB magnets of 6 mm height and 10 mm width having surface field ~ 3.5 kG placed on top of one another have been used to make the line cusp. The center to center separation between two adjacent line cusp is 4 cm. The source flange as shown

https://doi.org/10.1017/S0022377814001172 Published online by Cambridge University Press

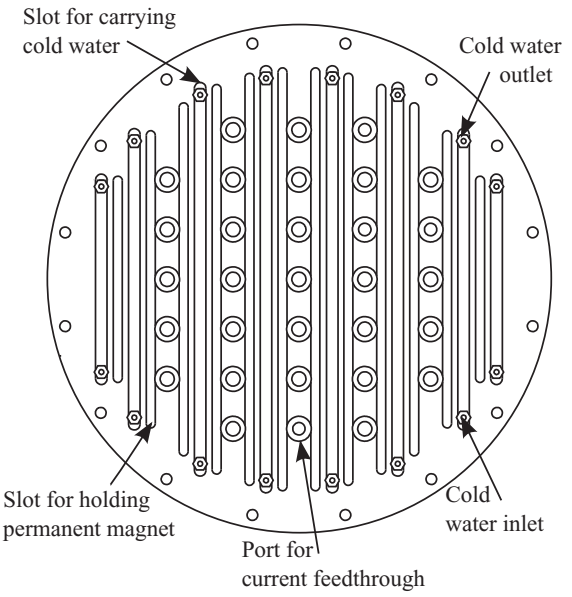


FIGURE 4. Plasma source flange.

in Fig. 4 is water cooled to ensure that the temperature of the NdFeB magnets used never crosses 80 °C which is the maximum operating temperature for the magnets.

For regular operations, 90 tungsten filaments of equal length and diameter of 0.125 mm, placed at a distance of $\sim$ 21.3 cm from the inner wall of the source flange arranged in the form of a matrix are used to produce the plasma. For lower density operations number of filaments in the plasma source may be reduced to 47. The filament to filament separation is maintained at a distance less than twice the Larmor radius of the primary electrons in the region near the filament location. All the filaments are electrically connected parallel to one another.

5.2. *Vacuum vessel*

As seen in the schematic diagram of IMPED (Fig. 5) the device is 3.38 m long having three stainless steel chambers: source chamber, source chamber extension and main plasma chamber. The source chamber is 0.5 m in diameter and 0.5 m in length whereas the source chamber extension is 0.346 m in diameter and 0.62 m in length. The main plasma chamber is composed of five sub-chambers, each having a diameter of 0.16 m. Out of the five subchambers, four subchambers together have a total length of 1.9 m and is electrically isolated from the rest of the vacuum vessel. There is provision for attaching electrically isolated meshes between the source chamber and the source chamber extension and/or the source chamber extension and the main chamber. The meshes may be biased to alter the parameters of the plasma. The vacuum pumping system comprises of three pumps. One 700 $l\,s^{-1}$ diffusion pump and one 200 $l\,s^{-1}$ turbo molecular pump (TMP) are connected to diametrically opposite ports of the source chamber and aligned vertically whereas one 500 $l\,s^{-1}$ diffusion pump is connected to the other end of the device. The base pressure of the system obtained is 2×10^{-6} mbar.

5.3. *Magnet system*

The magnet system of IMPED is composed of three types of water cooled electromagnets, 'regular' magnets, 'extension' magnets and 'compensation' magnets,

https://doi.org/10.1017/S0022377814001172 Published online by Cambridge University Press

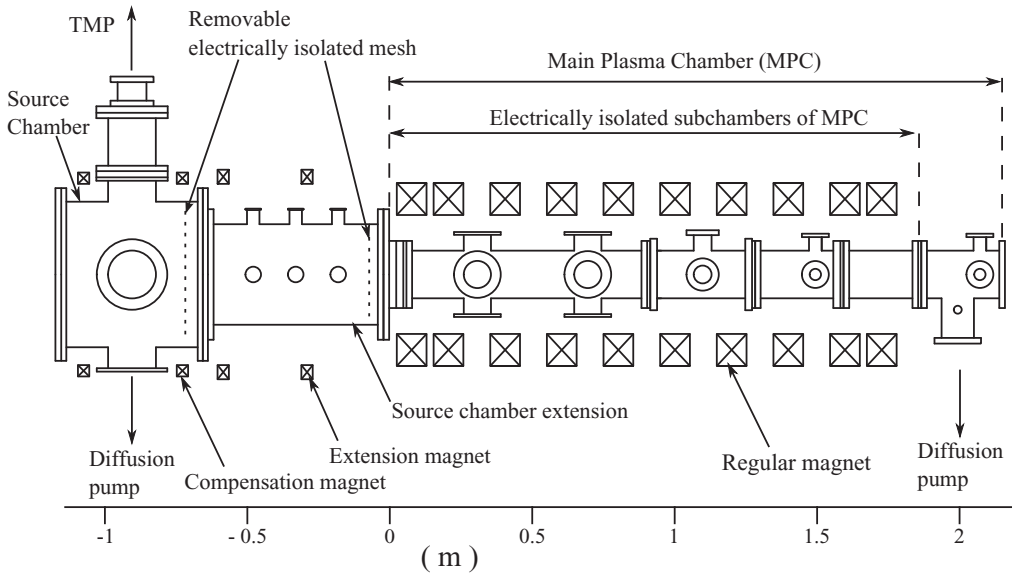


FIGURE 5. Schematic of the IMPED.

arranged coaxially with the vacuum vessel. Inner and outer diameter of regular magnets is 42 cm and 64.5 cm respectively. Thickness of the regular magnets along the axis is 10.5 cm. Each regular magnet has 120 turns. The regular magnets are used to produce a uniform flat top magnetic field over a distance of 1.3 m in the main plasma chamber. As per measurement with a Hall probe sensor, the axial magnetic field ripple within the flat top region is $\sim 0.7\%$. The magnetic field variation in the radial direction within 8 cm radius about the axis is $\sim 0.46\%$ in the flat top region. The separation between two consecutive regular magnets is 9.5 cm, while the last two regular magnets at either end are separated by 2.5 cm. The maximum magnetic field that can be attained in the main chamber using the regular magnets and the current set of power supplies over the flat top is 1.2 kG.

The other two types of electromagnets, the extension and the compensation magnets are used to maintain the magnitude of the magnetic field near the emitting filaments at permissible level irrespective of the magnetic field in the main chamber. The compensation magnets and the extension magnets are arranged coaxially around the source chamber and the source chamber extension respectively. The inner diameter and length along the axis of both the compensation and extension magnet are 64 cm and 4.5 cm, while the outer diameter of the compensation and the extension magnet are 72.4 cm and 74.8 cm respectively. The magnetic field profile of the magnet system is shown in the Fig. 6.

The magnet system of IMPED allows one to change the magnetic field in the source chamber near filaments without altering the magnetic field in the main chamber. The regular magnets of IMPED are powered by four different power supplies, depending on experimental requirement different current can be passed through different regular coils to establish gradients in the main chamber. It must also be noted that keeping the experimental flexibility in mind two extension magnets and the two compensation magnets are powered by four different power supplies. This facility will enable one to achieve wide variation in the magnetic field profile in transition region between the source and the main plasma chamber.

https://doi.org/10.1017/S0022377814001172 Published online by Cambridge University Press

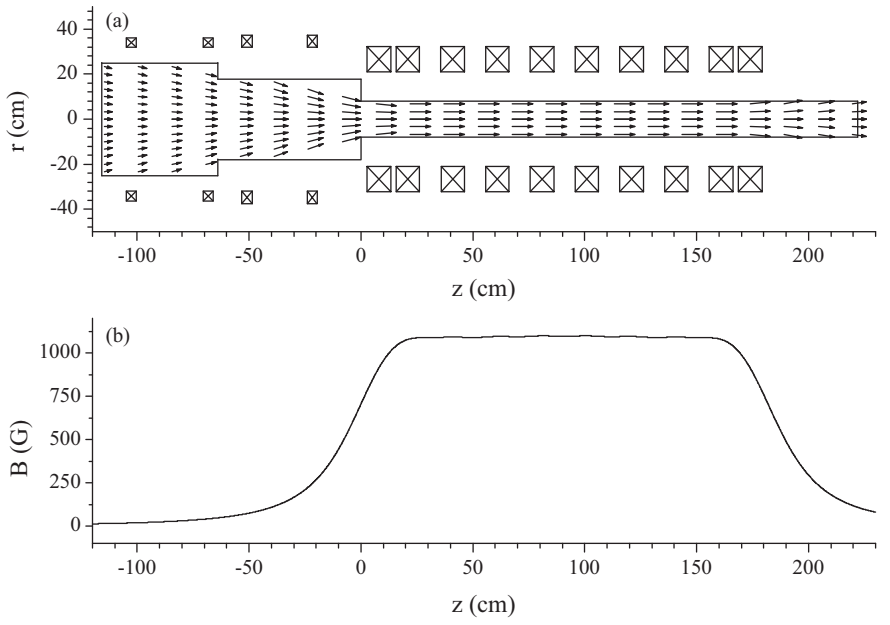


FIGURE 6. (a) Profile of the magnetic field produced by the regular magnets. The length of the arrows is proportional to $log|\vec{B}|$ (b) Variation of the magnetic field along axis for NI = 18000 ampturns in the regular magnets.

5.4. *Diagnostic*

Single Langmuir probes are used for carrying out axial and radial measurements of plasma density and electron temperature. The stroke length of the axial Langmuir probe is 1.7 m. A code is developed in MATLab for quick processing of the obtained Langmuir probe data. Additionally other electric probes available for making measurements are double probe, triple probe, emissive probe and rack probe. Facility for optical emission spectroscopy is also available for experiments. Single gridded exciter is used for exciting disturbances in the ion time scale. The Langmuir probes are used for receiving the signals. In addition to the phase mixing experiment involving an ion wave background, ion acoustic wave is used as an additional diagnostic tool for cross verification of the temperature measured using Langmuir probe.

For exciting and detecting plasma oscillation/electron plasma wave two schemes are designed. The first scheme employs three gridded exciters (Derfler and Simonen 1967) for exciting and detecting signals in the electron time scale. The central grid is the power grid and the outer two grids are to be grounded to reduce the capacitive pick up between the exciter and receiver. In the second scheme, a tungsten wire fed directly from a 50 Ω coaxial line is to be used for exciting Langmuir wave (Barrett et al. 1968) and another tungsten wire is to be used for detection. To reduce the direct pick up between the exciter and receiver a stainless steel cylinder of continuous length 1 m will be placed in the main chamber and both the exciting and receiving probes will be inside the cylinder. The cylinder will act as high pass filter and the experiment will be conducted below the cut off frequency. Plasma oscillation/electron plasma wave circuit will be used for excitation of linear wave and nonlinear electron plasma wave for experimental investigation of phase mixing. In addition linear electron plasma wave will serve as diagnostic for determining density using the dispersion relation of the wave mode. Electrons are expected to be accelerated by phase mixing and wave

https://doi.org/10.1017/S0022377814001172 Published online by Cambridge University Press

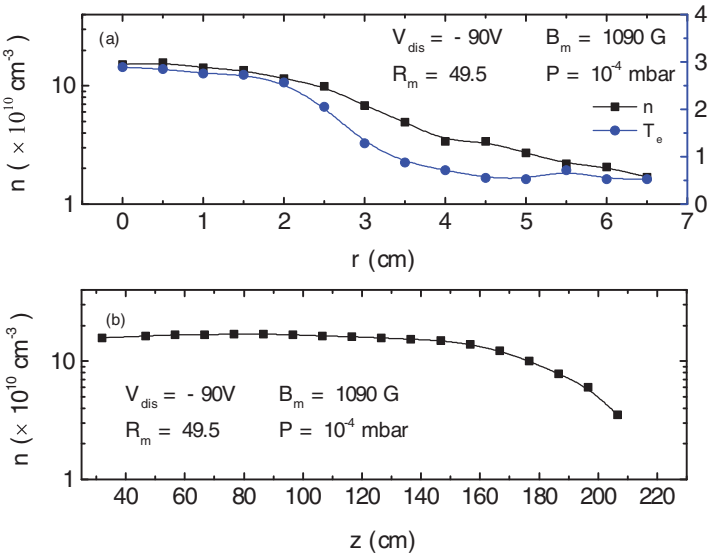


FIGURE 7. (a) Radial profile of density and temperature in the flat top region of the magnetic field in the main plasma chamber. (b) Axial variation of density in the main plasma chamber.

breaking of plasma oscillation/wave. These energetic electrons will be detected by a gridded energy analyzer.

As an alternate measurement of electron density a microwave interferometer system using heterodyne principle is being installed for on-line cord averaged density measurement.

5.5. *Initial results*

Quiescent, collisionless, magnetized, uniform plasma has been produced in IMPED. Initial plasma characterization in IMPED has been carried out in argon plasma using 90 filaments. The plasma produced is axially and radially uniform. The diameter of the uniform plasma as shown in Fig. 7(a) in the flat top magnetic field region of the main plasma chamber is 4 cm when the magnetic field in the main chamber and in the location of the filaments is 1090 G and 22 G, respectively.The axial uniformity of the plasma as shown in Fig. 7(b) extends over 120 cm in the main plasma chamber. The lowest operating pressure achieved is 1.7×10^{-5}mbar. The plasma density and temperature has been varied over range of $\sim 10^{9}$–10^{12} cm^{-3} and 2–5 eV respectively by varying operating pressure, axial magnetic field, filament heating current and mirror ratio R_m. R_m is the ratio of magnetic field in the main chamber B_m to that near filament electron source B_s (Bose et al. 2014).

R_m can be varied by changing the magnetic field near the filament electron source (B_s) keeping the magnetic field in the main chamber (B_m) constant. The plasma density in the main chamber is seen to change by varying R_m and this is an important knob available for our experiment. This feature enhances the range of densities accessible for a given operating pressure and magnetic field in the main chamber. Figure 8(a) shows the decrease in density by a factor $\sim$4.3 in the uniform magnetic field region of the main chamber ($B_m = 1090$ G) by increasing R_m from 50 to 570 at discharge voltage of -90 V and argon pressure of 5×10^{-5} mbar. The variation of the discharge current with R_m is shown in Fig. 8(b); the discharge current is seen to follow the density variation. The reason for this reduction in density may be because

https://doi.org/10.1017/S0022377814001172 Published online by Cambridge University Press

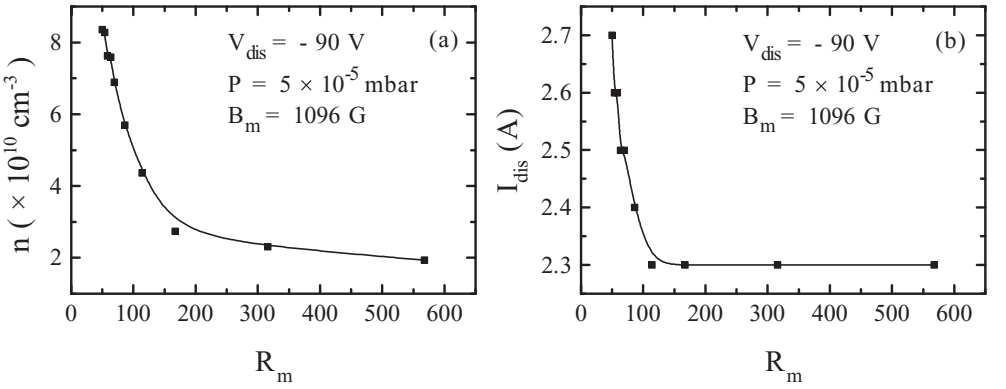


FIGURE 8. Variation of density and discharge current with mirror ratio.

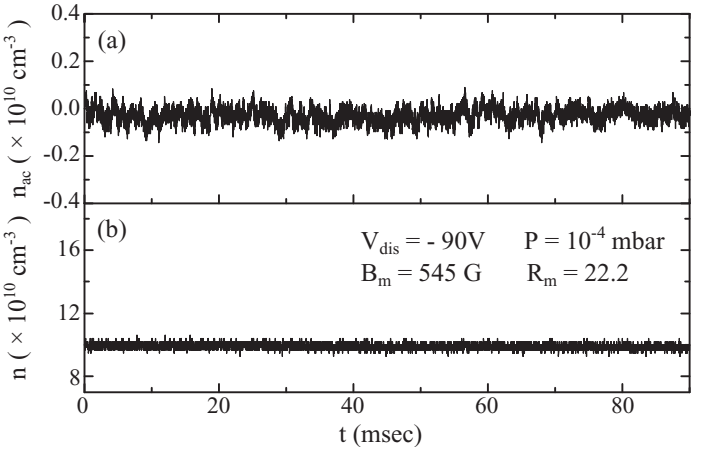


FIGURE 9. (a) Variation of the ac component of the density with time. (b) Variation of the total density with time.

of enhanced radial diffusion of plasma in the source region at lower values of axial magnetic field there with high R_m.

The quiescence of plasma is estimated from the ion saturation current. It is interpreted as the ratio of the root mean square value of the ac component (time varying noise component) of the density and the mean density. A quiescency of $\delta n_{noise}/n \sim 0.005$ is achieved at -90 V discharge voltage and 10^{-4}mbar filling pressure, 545 G magnetic field in the main chamber and $R_m = 22.2$. Figures 9(a) and (b) demonstrate the temporal variation of the background noise component of density (n_{ac}) and the mean density, respectively for the above mentioned parameters.

Besides steady state operation IMPED can also be operated in pulsed mode by switching off the biasing voltage of the multifilamentary discharge. This option is useful for wave studies due to the absence of non-thermal electrons in afterglow plasma. The variation of density with time in afterglow mode for a plasma produced with discharge voltage -80 V, magnetic field in the main chamber of 1090 G, $R_m = 49.5$ and operating pressure 10^{-4} mbar is shown in Fig. 10. This measurement is carried out at $r = 0$ cm in the uniform magnetic field region of the main plasma chamber. The density e-folding time is $\sim 316\,\mu$sec. This time is sufficient for carrying out phase mixing of nonlinear oscillation experiment, as the phenomenon is expected to occur within few periods of plasma oscillations, that is within 1 μsec.

https://doi.org/10.1017/S0022377814001172 Published online by Cambridge University Press

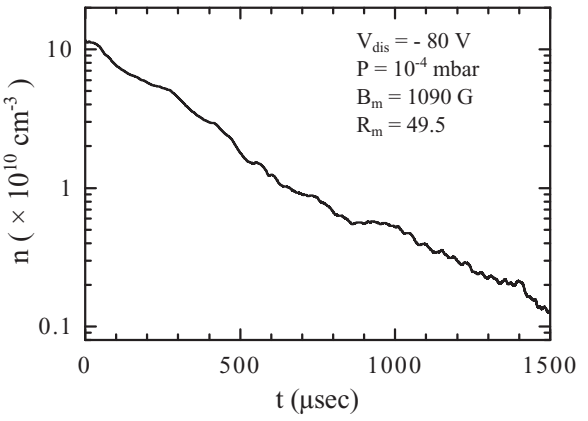


FIGURE 10. Variation of density with time in afterglow operation.

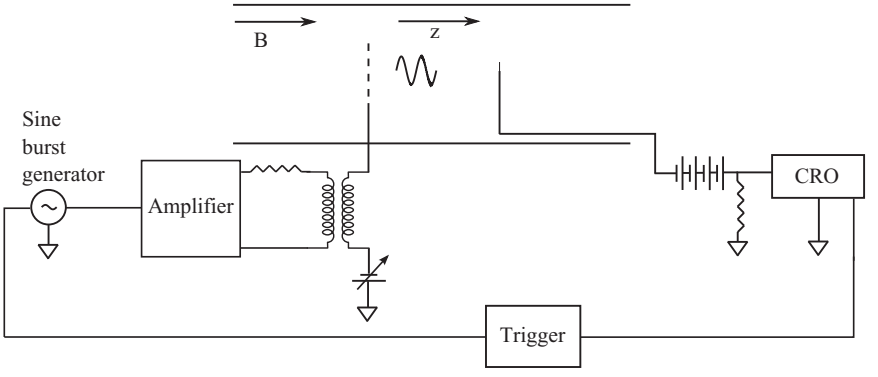


FIGURE 11. Schematic of ion wave exciter.

The initial goal is to study the phase mixing of nonlinear plasma oscillation in the presence of an ion wave in the background. The basic requirement for the experiment is a long uniform plasma column at 10^{-4} mbar pressure which has already been achieved. The initial effort is concentrated in excitation and detection of an ion wave. It shall be followed by excitation and detection of plasma oscillation/wave in the presence of an ion wave in the background.

Disturbance in the ion time scale is excited by applying a oscillating voltage to a 30 mm diameter stainless steel (SS304) mesh having a wire of diameter 0.26 mm and 0.9 mm aperture. The circuit being used for exciting and detecting ion wave is shown in Fig. 11. The initial wave propagation data are shown in Fig. 12, which depicts Langmuir probe receiver signals at four axial locations when the exciter is energized with a single burst voltage pulse. The data is acquired at 1×10^{-4} mbar , -70 V discharge voltage, $R_m = 49.5$ and 327 G magnetic field in the main chamber. The propagation speed of the observed peak is found to be 2.6×10^5 cms^{-1} which is close to the ion acoustic speed estimated from the plasma parameters.

6. Discussion and future plan

To study the phenomena of phase mixing and wave breaking of plasma oscillation in a controlled manner a new machine, IMPED, has been designed and constructed and presently ready for operation. The parameter regime of its operation has been

https://doi.org/10.1017/S0022377814001172 Published online by Cambridge University Press

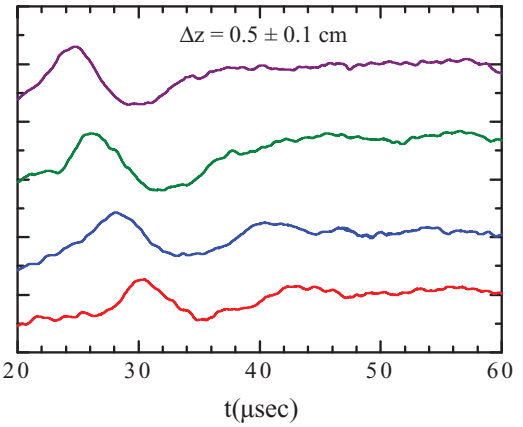


FIGURE 12. Propagation of disturbance in the ion time scale.

explored and found to be suitable for studying the phenomena which demand challenging requirements on different plasma features, namely, quiescency, uniformity, collisionality, plasma density, operating pressure, etc. A preliminary experiment on launching ion acoustic wave to create a non-uniform plasma density background for the experiment of phase mixing of plasma oscillation has been conducted successfully. The first result of phase mixing of plasma oscillations is expected to be published in six to twelve months. The IMPED machine is made reasonably flexible in nature and allows easy modifications/upgrades. So, in addition to the experiments we have discussed and planned to be carried out in this machine in the current configuration, experimental studies of Bernstein wave, upper hybrid wave, Alfven wave and magnetic reconnection may also be performed following some upgrades of the present main plasma chamber. Mainly, it will be replaced by a 30 cm diameter and 250 cm long main chamber. The diameter of the source chamber will also be increased to 1 m.

REFERENCES

Barrett, P. J., Jones, H. G. and Franklin, R. N. 1968 Dispersion of electron plasma waves. *Plasma Phys.* **10**(10), 911.

Bauer, B. S., Wong, A. Y., Decyk, V. K. and Rosenthal, G. 1992 Experimental observation of superstrong electron plasma waves and wave breaking. *Phys. Rev. Lett.* **68**, 3706–3709.

Boeschoten, F. and Schwirzke, F. 1962 Investigation of a stationary plasma in a magnetic field. *Nucl. Fusion* **2**(1–2), 54.

Bose, S., Kaur, M., Chattopadhyay, P. K., Ghosh, J. and Saxena, Y. C. 2014 Imped – a new magnetized linear plasma device with wide operating range. Manuscript submitted.

Botha, G., Arber, T., Nakariakov, V. M. and Keenan, F. P. 2000 A developed stage of alfven wave phase mixing. *Astron. Astrophys.* **363**(3), 1186–1194.

Chen, F. F. 1962 *Production of Laboratory Plasmas, Plasma Physics: Summer Institute, Princeton University, 1962 : Lecture Notes*. Trustees of Princeton University.

Coffey, T. P. 1971 Breaking of large amplitude plasma oscillations. *Phys. Fluids (1958–1988)* **14**(7), 1402–1406.

Davidson, R. C. 1972 *Methods in nonlinear plasma theory*, Academic Press, New York.

Dawson, J. 1961 On landau damping. *Phys. Fluids (1958–1988)* **4**(7), 869–874.

Dawson, J. 1962 One dimensional plasma model. *Phys. Fluids (1958–1988)* **5**(4), 445–459.

Dawson, J. M. 1959 Nonlinear electron oscillations in a cold plasma. *Phys. Rev.* **113**, 383–387.

Derfler, H. and Simonen, T. C. 1967 Experimental verification of landau waves in an isotropic electron plasma. *J. Appl. Phys.* **38**(13), 5014–5020.

https://doi.org/10.1017/S0022377814001172 Published online by Cambridge University Press

Esarey, E., Schroeder, C. B. and Leemans, W. P. 2009 Physics of laser-driven plasma-based electron accelerators. *Rev. Mod. Phys.* **81**, 1229–1285.

Franklin, R. N., Hamberger, S. M., Lampis, G. and Smith, G. J. 1975a Nonlinear behaviour of a finite amplitude electron plasma wave. i. electron trapping effects. *Proc. R. Soc.* A **347**(1648), 1–24.

Franklin, R. N., Hamberger, S. M., Lampis, G. and Smith, G. J. 1975b Nonlinear behaviour of a finite amplitude electron plasma wave. ii. wave-wave interactions. *Proc. R. Soc.* A **347**(1648), 25–46.

Franklin, R. N., MacKinlay, R. R., Edgley, P. D. and Wall, D. N. 1978 Nonlinear behaviour of a finite amplitude electron plasma wave. iii. the sideband instability. *Proc. R. Soc.* A **360**(1701), 229–242.

Gekelman, W. and Stenzel, R. L. 1975 Large, quiescent, magnetized plasma for wave studies. *Rev. Sci. Instrum.* **46**(10), 1386–1393.

Infeld, E. and Rowlands, G. 1990 Langmuir oscillations against a single-ion pulse or cavity background. *Phys. Rev.* A **42**, 838–842.

Infeld, E., Rowlands, G. and Torvén, S. 1989 Ion density cavities can cause nonlinear plasma oscillations to peak. *Phys. Rev. Lett.* **62**, 2269–2272.

Kaw, P. K., Lin, A. T. and Dawson, J. M. 1973 Quasiresonant mode coupling of electron plasma waves. *Phys. Fluids* **16**(11), 1967–1975.

Kodama, R et al. 2001 Fast heating of ultrahigh-density plasma as a step towards laser fusion ignition. *Nature* **412**(6849), 798–802.

Landau, L. 1946 On the vibrations of the electronic plasma. *J. Phys.* **10**, 25–34.

Limpaecher, R. and MacKenzie, K. R. 1973 Magnetic multipole containment of large uniform collisionless quiescent plasmas. *Rev. Sci. Instrum.* **44**(6), 726–731.

Malmberg, J. H., Wharton, C. B. and Drummond, W. E. 1966 Lanadau damping of electron plasma waves. In: *Proc. Conf. Plasma Physics and Controlled Nuclear Fusion Research*, International Atomic Energy Agency, Vienna, pp. 485–497.

Malmberg, J. H. and Wharton, C. B. 1967 Collisionless damping of large-amplitude plasma waves. *Phys. Rev. Lett.* **19**, 775–778.

Modena, A. et al. 1995 Electron acceleration from the breaking of relativistic plasma waves. *Nature* **377**, 606–608.

de Nicola, S. and Nappi, C. 1992 Collisional drag can prevent plasma oscillations from breaking. *EPL Europhys. Lett.)* **19**(5), 381.

O'Neil, T. 1965 Collisionless damping of nonlinear plasma oscillations. *Phys. Fluids (1958–1988)* **8**(12), 2255–2262.

Rynn, N. and D'Angelo, N. 1960 Device for generating a low temperature, highly ionized cesium plasma. *Rev. Sci. Instrum.* **31**(12), 1326–1333.

Sengupta, S., Kaw, P., Saxena, V., Sen, A. and Das, A. 2011 Phase mixing/wave breaking studies of large amplitude oscillations in a cold homogeneous unmagnetized plasma. *Plasma Phys. Control. Fusion* **53**(7), 074 014.

Sengupta, S. and Kaw, P. K. 1999 Phase mixing of nonlinear plasma oscillations in an arbitrary mass ratio cold plasma. *Phys. Rev. Lett.* **82**, 1867–1870.

Tabak, M., Hammer, J., Glinsky, M. E., Kruer, W. L., Wilks, S. C., Woodworth, J., Campbell, E. M., Perry, M. D. and Mason, R. J. 1994 Ignition and high gain with ultrapowerful lasers*. *Phys. Plasmas (1994–present)* **1**(5), 1626–1634.

Tajima, T. and Dawson, J. M. 1979 Laser electron accelerator. *Phys. Rev. Lett.* **43**, 267–270.

Tonks, L. and Langmuir, I. 1929 Oscillations in ionized gases. *Phys. Rev.* **33**, 195–210.

Verma, P. S., Sengupta, S. and Kaw, P. 2012 Residual bernstein-greene-kruskal-like waves after one-dimensional electron wave breaking in a cold plasma. *Phys. Rev. E* **86**, 016 410.

Wharton, C. B., Malmberg, J. H. and O'Neil, T. M. 1968 Nonlinear effects of large-amplitude plasma waves. *Phys. Fluids (1958–1988)* **11**(8), 1761–1763.

https://doi.org/10.1017/S0022377814001172 Published online by Cambridge University Press